LA--12102

DE91 015977

An Investigation of Dual-Mode Operation of a Nuclear-Thermal Rocket Engine

William L. Kirk
James C. Hedstrom
Stanley W. Moore
Robert D. McFarland
Michael A. Merrigan
John J. Buksa
Michael W. Cappiello
Donald L. Hanson
Keith A. Woloshun

LOS ALAMOS Los Alamos National Laboratory
Los Alamos,New Mexico 87545

CONTENTS

ABSTRACT 1
I. INTRODUCTION AND BACKGROUND 1
II. FLOW CONFIGURATIONS 8
A. The Direct Flow Path 8
B. The Tie-Tube Flow Path 10
C. Special Unfueled Elements 17
D. In-Core Heat Pipes 19
III. SYSTEM ANALYSIS 26
IV. SUMMARY AND CONCLUSIONS 32
REFERENCES 34

FIGURES

1. Cross section of a typical Rover reactor 3
2. End view of 19-hole composite-matrix fuel element 3
3. Support element geometry 4
4. Cluster of fuel and support elements and hot-end support hardware 5
5. Example of an overall engine flow scheme 6
6. Open-cycle flow paths diagram 8
7. Strength vs temperature for selected materials 9
8. Calculated maximum fuel temperatures for several values of power per tie tube with moderator in the support element, hydrogen coolant 11
9. Calculated maximum fuel temperatures for several values of power per tie tube with no moderator in the support element, hydrogen coolant 11
10. Calculated maximum fuel temperatures for several values of power per tie tube with no moderator in the support element, helium coolant 12
11. Tie-tube exit gas temperatures for case of Fig. 8 12
12. Maximum tie-tube temperatures for case of Fig. 8 13
13. Tie-tube exit gas temperatures for case of Fig. 9 13
14. Maximum tie-tube temperatures for case of Fig. 9 14
15. Tie-tube exit gas temperatures for case of Fig. 10 14
16. Maximum tie-tube temperatures for case of Fig. 10 15
17. Calculated maximum fuel temperatures with hydrogen in gaps compared with Fig. 10 16

18. Estimate of the thermal radiation from the surface of an aluminum or a titanium pressure vessel 16
19. Block diagram of external region cooling in series with the tie tubes and periphery cooling 18
20. Block diagram of separate cooling circuit for external regions 18
21. Maximum fuel temperatures using special elements at various closed-cycle power levels, hydrogen coolant 20
22. Special element exit gas temperatures for Fig. 21 cases 20
23. Maximum fuel temperatures using special elements at various closed-cycle power levels, helium coolant 21
24. Special element exit gas temperature for Fig. 23 cases 21
25. Block diagram of flow paths using special elements and parallel cooling of other reactor regions 22
26. Block diagram of flow paths using special elements and series cooling of other reactor regions 22
27. Performance limit curves for heat pipe 26
28. Brayton component mass as a function of electric power level 29
29. Brayton cycle power-conversion subsystem mass as a function of electric power level and turbine inlet temperature 30
30. Mass comparison of 10-MWe dual-mode and independent nuclear propulsion/power systems 34

TABLES

I-A. Lithium Heat Pipe Input for HTPIPE 24
I-B. Summary of Output Generated by HTPIPE 25
II. Component Specific Masses for a 10-MWe Man-Rated Power System 29
III. Assumptions Used to Calculate Component Masses for Dual-Mode and Independent Nuclear Propulsion/Power Systems 32
IV. Component Comparison of Dual-Mode and Independent Propulsion/Power Systems 33

AN INVESTIGATION OF DUAL-MODE OPERATION OF A NUCLEAR-THERMAL ROCKET ENGINE

by

William L. Kirk, James C. Hedstrom, Stanley W. Moore, Robert D. McFarland, Michael A. Merrigan, John J. Buksa, Michael W. Cappiello, Donald L. Hanson, and Keith A.Woloshun

ABSTRACT

A preliminary assessment of the technical feasibility and mass competitiveness of a dual-mode nuclear propulsion and power system based on Rover-type reactors has been completed. Earlier studies have indicated that dual-mode systems appear attractive for electrical power levels of a few kilowatts. However, at the megawatt electrical power level considered in this study, it appears that extensive modifications to the nuclear-thermal engines would be required, the feasibility of which is unclear. Mass competitiveness at high electrical power levels is also uncertain. Further study of reactor and shield design in conjunction with mission and vehicle studies is necessary in order to determine a useful dual-mode power range.

I. INTRODUCTION AND BACKGROUND

The Space Exploration Initiative that was set in motion by President Bush in July 1989 includes a manned mission to Mars. This ambitious mission is an ideal application for nuclear propulsion, using either nuclear-thermal engines, in which hydrogen is heated by a nuclear reactor and then expanded through a nozzle to produce a high-velocity expellant, or nuclear-electric engines, in which thermal energy from the reactor is converted to electricity that powers an ion or plasma thruster. Furthermore, there is a possibility of advantageously combining these two propulsive modes, using the high-thrust, moderately high-specific-impulse (Isp) nuclear-thermal mode for propulsive maneuvers near Earth and Mars, where the high thrust is important because of the large gravity effects, and using the very high Isp, low-thrust nuclear-electric engine during the trip between the two planets. The potential advantage is a reduction in the initial mass in earth orbit required for the mission and/or a reduction in trip time. For the purposes of this study, we assume that the combination is advantageous. Our purpose is to explore alternative configurations for providing both kinds of propulsion. In particular, we will examine the use of a single reactor to both heat hydrogen to extremely high temperatures in the open-cycle (nuclear-thermal propulsion) mode and to heat one of a variety of fluids in the closed-cycle (nuclear-electric propulsion) mode. The alternative is to use two reactors, one for each mode of operation. There are two issues in

choosing between a dual-mode reactor and two separate reactors. One is the feasibility of a dual-mode reactor at the desired power and operating time; the other is whether the dual-mode configuration provides a mass reduction compared with the two-reactor configuration. Section II of this report deals with the first issue and Sec. III deals with the second issue.

As a basis for the dual-mode reactor analysis, we use the reactor configurations developed by Los Alamos during the Rover Program, the national nuclear rocket program of 1955-1972. The Los Alamos role in the Rover Program was the development of the nuclear rocket propulsion reactor technology; the role of the major industrial contractors (an engine contractor, Aerojet-General Corporation, and a reactor subcontractor, Westinghouse Astronuclear Laboratory) was to adapt this technology to the development of a flight-qualified engine, the Nuclear Engine for Rocket Vehicle Applications (NERVA) engine. Although the program was terminated before the completion of engine development, major technical achievements, including the testing of 20 reactors at the Nuclear Rocket Development Station in Nevada, demonstrated the soundness of the basic reactor configuration.

A cross section of a typical Rover reactor is shown in Fig. 1. The reactor core consists of an array of hexagonal elements, 0.753 in. across flats and approximately 52 in. long. Most of the elements, as many as six out of seven, are fuel elements, pierced with nineteen, 0.1-in.-diam axial coolant passages (see Fig. 2). The fuel elements consist of either graphite containing uranium carbide particles or, as shown in Fig. 2, a composite of UC•ZrC solid solution and graphite. [Limited work was done on pure carbide (UC-ZrC) fuel, which is likely to require a different fuel geometry.] All surfaces of the fuel element are coated with ZrC to reduce corrosion by the hot hydrogen. One-seventh or more of the core elements contain no uranium and house a cooled support structure that extends the entire length of the reactor core. The support element geometry is shown in Fig. 3 and a cluster of fuel and support elements in Fig. 4. The support element configuration depicted in Fig. 3 provides for regenerative cooling of the support hardware; that is, low-temperature H_2 enters the support element at the inlet end of the reactor core, passes through the inner flow passage to the hot end of the core, and returns to the inlet end of the core through the outer flow annulus.

Eventually this hydrogen, perhaps after being used to drive the engine turbopump, returns to the core inlet to pass through the fuel elements. (See Fig. 5 for one example of an overall engine flow scheme.) Regenerative cooling of the support structure maximizes engine Isp by reducing or eliminating bypass flow of cool H_2 into the nozzle chamber. This regenerative circuit is referred to as the tie-tube circuit. It has a potentially important role in extracting heat from the reactor core in

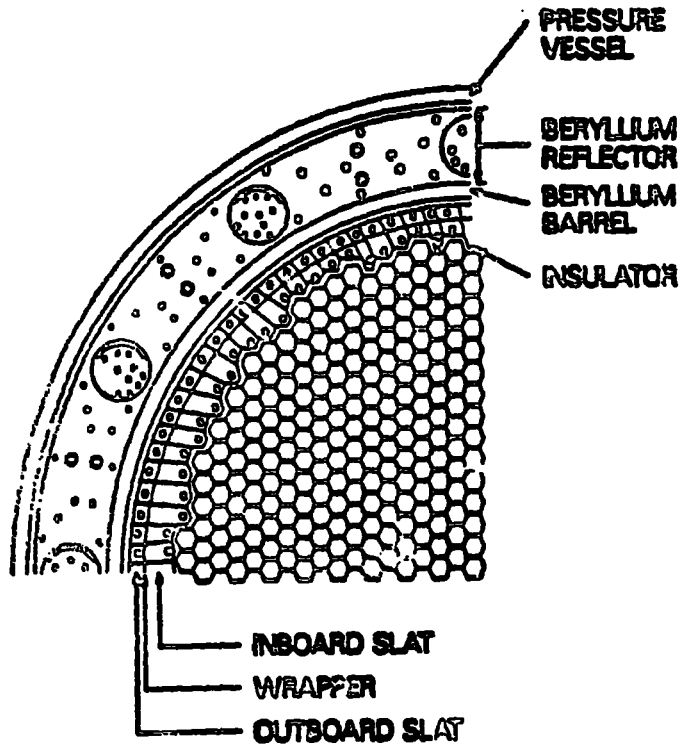

Fig. 1.

Cross section of a typical Rover reactor.

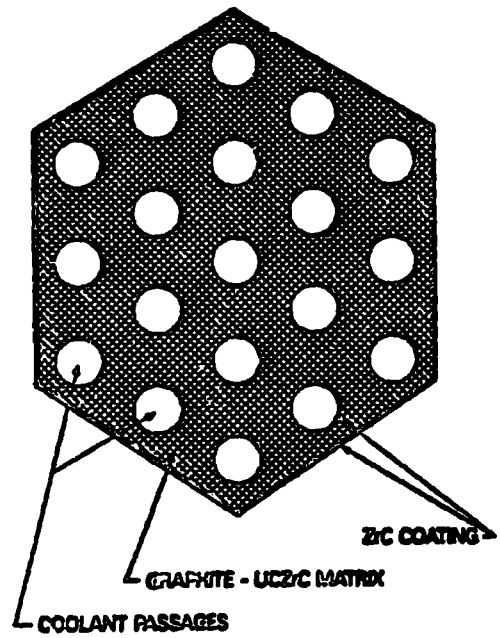

Fig. 2.

End view of 19-hole composite-matrix fuel element.

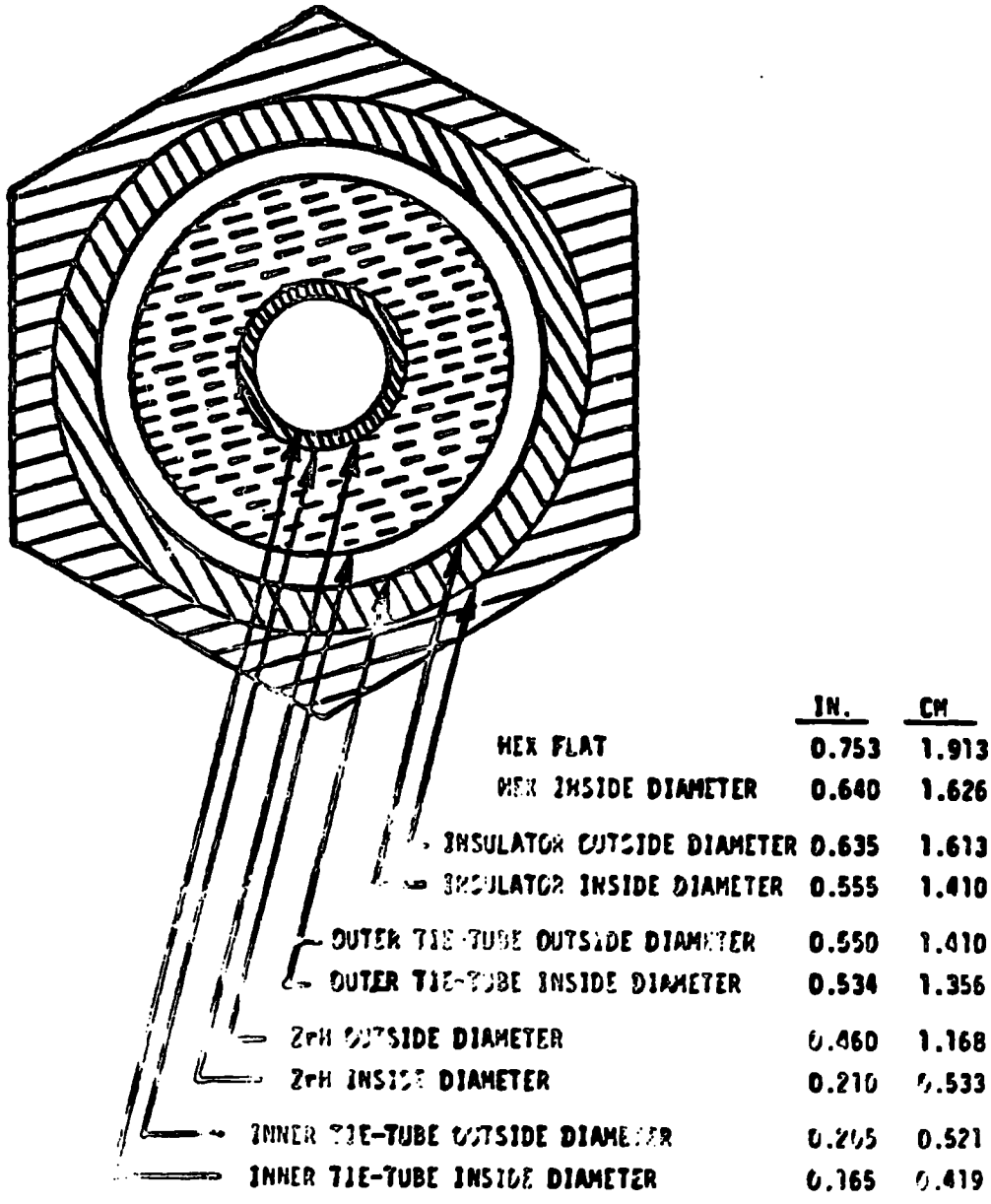

Fig. 3.
Support element geometry.

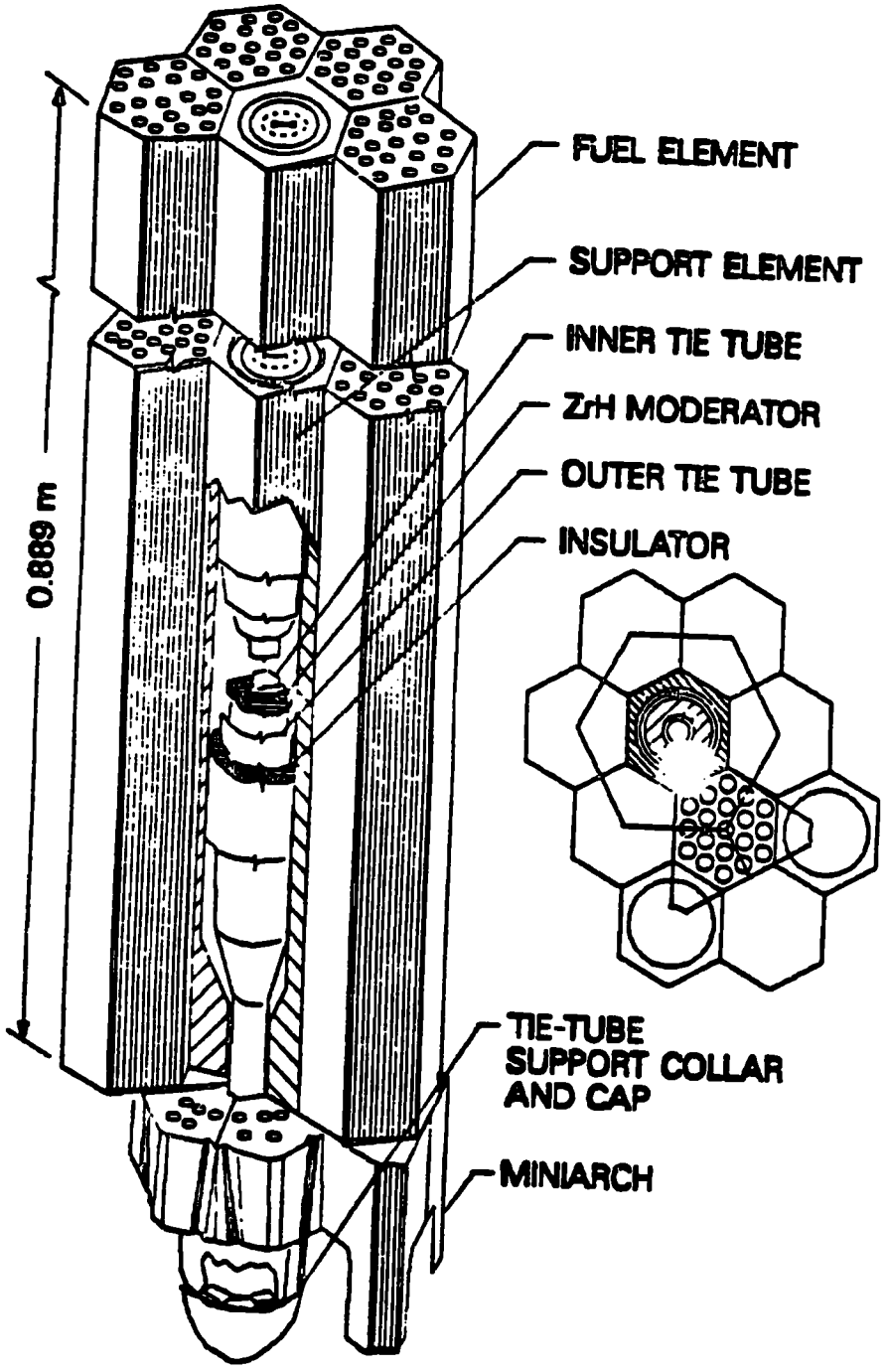

Fig. 4.
Cluster of fuel and support elements and hot-end support hardware.

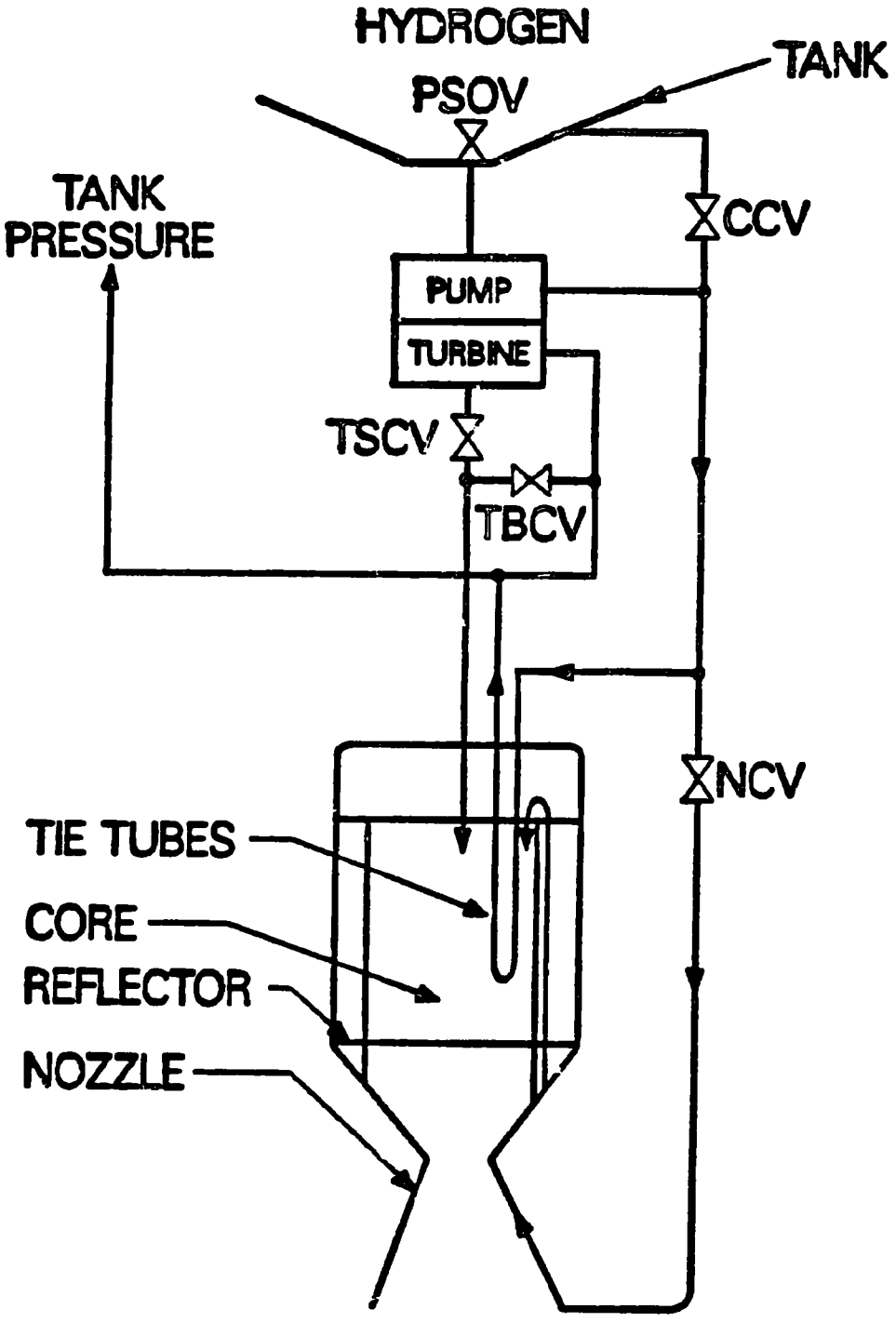

Fig. 5.
Example of an overall engine flow scheme.

the closed-cycle phase of the dual-mode concept. Regenerative cooling is also attractive for low-temperature components at the reactor core periphery, a fact we will also use in the analysis that follows.

The support element version shown in Fig. 3 also contains zirconium hydride to provide neutron moderation. The zirconium hydride was originally incorporated to reduce the reactor size required for nuclear criticality so that lower-thrust engines would be feasible. However, it seems likely that incorporating the moderator in the support elements will prove to be advantageous for larger reactors such as the 1500-MW size used as the basis for the present study. A better-moderated reactor needs less uranium, which should increase the temperature capability of the fuel. In subsequent sections, we will consider support elements both with and without zirconium hydride.

There are a number of possible fluid flow schemes that need to be considered for closed-cycle heat removal from the reactor. To aid in the visualization of several alternatives that we have considered, we will use variations of the quasi-block diagram shown in Fig. 6. The diagram in Fig. 6 shows the reactor-nozzle assembly internal flow paths used during open-cycle operations. These internal circuits can be connected in different ways even for open-cycle operation; for example, the H_2 exiting from the tie tubes and periphery may be used to drive the engine turbine—or all of the H_2 flow from the reflector, tie tubes, and periphery may be collected to drive the turbine before entering the reactor core. The choice depends on turbopump power needs and the power available from the tie tubes and periphery. Also, Fig. 6 is arranged to indicate some of the thermal coupling between reactor regions, such as the conduction of heat from the fuel elements to tie tubes and periphery, and the potential for thermal conduction/radiation between core periphery and reflector and between the reflector and pressure vessel.

A 75,000-lb-thrust engine requires about 1500 MW of reactor thermal power; we assume that 5-10 MWe, thus 20-100 MWt, are needed for the electric propulsion mode. We will use 30 MWt as a nominal reactor power for closed-cycle operation.

We will point out without much elaboration that 30 MWt for 330 days is 10,000 MW days, which burns 10 kg of U^{235}. Total fuel loadings for a 1500-MW Rover reactor were about 200 kg. We have no data for 5% burnup in Rover fuels. Maximum burnup in Rover reactor tests was about 0.01%.

Another possibly important consequence of dual-mode operation that we have not analyzed quantitatively is a requirement for additional shielding. The reactor power integral for closed-cycle operation may be considerably larger that the open-cycle power integral. Furthermore, it is spread over a long time interval so that it is not feasible to use a heavily shielded "storm cellar," which might be advantageous for the brief open-cycle operation. Therefore, the increase in shield mass required for dual-mode operation may be quite large.

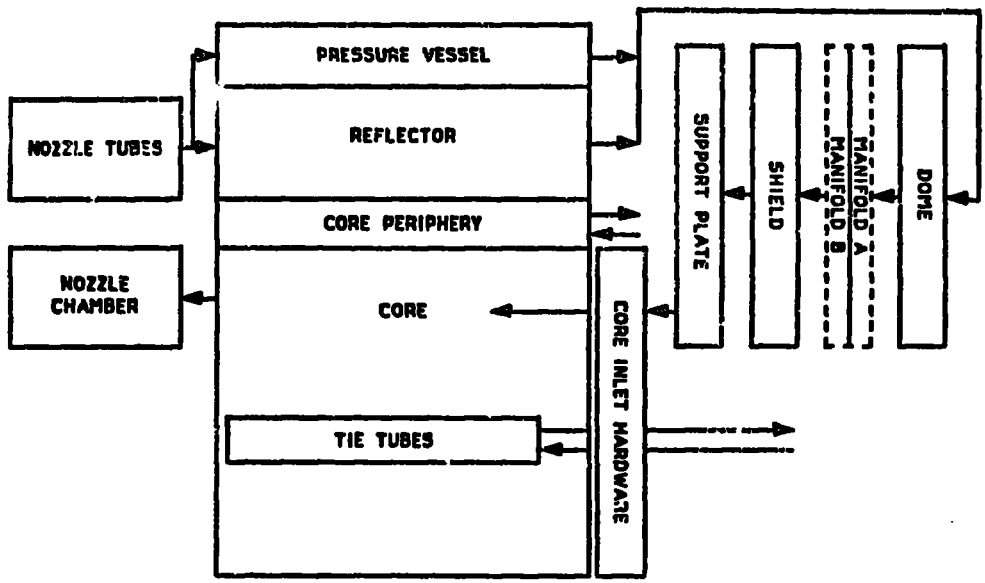

Fig. 6.
Open-cycle flow paths diagram.

II. FLOW CONFIGURATIONS

We will discuss the following possible closed-cycle heat removal flow schemes:

A. Direct flow path with blocked nozzle and a bypass port in the nozzle chamber. (Closed-cycle coolant removes heat from all reactor regions.)

B. Closed-cycle coolant path through tie tubes and periphery.
   1. In series with nozzle-pressure vessel-reflector.
   2. With parallel cooling of ex-core regions.

C. A special core element circuit.
   1. In series with other reactor regions.
   2. With parallel cooling of other reactor regions.

D. In-core heat pipes.

A. The Direct Flow Path

In this approach, we would allow the closed-cycle working fluid (probably helium or a helium-xenon mixture) to follow the same reactor flow path used in open-cycle operation (as shown in Fig. 6) as far as the nozzle chamber. Then, in order to close the loop, we would need to block the flow through the nozzle at some convenient nozzle station and, upstream of the block, open a valve that diverts the fluid into a duct passing between the nozzle cooling tubes and leading

to the energy-conversion system. The approach has two potential advantages: flow circuit simplicity and cooling of all reactor regions. However, there are major questions regarding the feasibility of blocking the nozzle in a leak-tight manner, removing the block during subsequent open-cycle operations, and, particularly, the feasibility of placing a port in the nozzle chamber that can survive during open-cycle operation at chamber temperatures approaching 3000 K or higher. Developing a plausible conceptual design for the nozzle closure/port combination is beyond the scope of the present study. Nuclear engine nozzle ports have been used for providing turbopump energy in bleed-cycle designs. Blocking the nozzle might be more practical if the engine is not required to return to the open-cycle mode.

There is one other concern. Because the radiator that rejects the waste heat from the electrical energy generation system is a major portion of the system mass, it is important to keep the radiator temperature high. This means that the inlet temperature to the reactor is much higher than during open-cycle operation. Consequently, materials such as aluminum that are attractive for the single-mode nuclear thermal rocket design are no longer usable in the dual-mode design, even in the direct flow path case. Figure 7 shows the behavior of several structural materials vs temperature. Without a detailed analysis, it is hard to judge the magnitude of the mass and

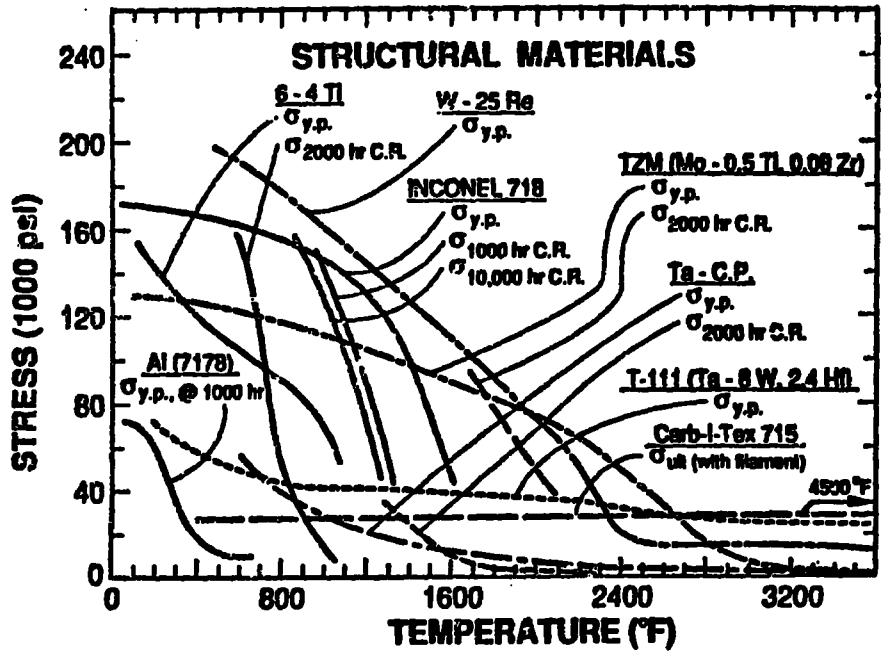

Fig. 7.
Strength vs temperature for selected materials.

neutronic penalties that might result; however, they are likely to be less for this alternative than for those discussed in subsequent sections. Consequently, the direct flow path may be the best approach for dual-mode design. However, much more work will be required to prove feasibility of this approach.

B. The Tie-Tube Flow Path

Beginning with an initial study by Beveridge,[1] several authors including Booth and Altsheimer,[2] and Layton, Grey, and Smith[3] have considered the use of the tie-tube circuit to extract heat from a nuclear rocket reactor core. In one sense the tie-tube circuit is ideally suited for this purpose because it provides an already existing closed path through the reactor core (see Fig. 6). If, as seems desirable, the core periphery also is cooled by a two-pass circuit, that circuit also could and should be used in parallel with the tie-tube circuit. both to provide additional coolant flow area and heat-transfer area and to cool an important reactor region.

Nearly all of the previous studies have focused on producing relatively low power in the closed-cycle mode, generally a few kilowatts. Booth and Altsheimer, for example, concluded that a 16,000-lb-thrust engine (approximately a 20-in.-diam core) would be limited to a maximum closed-cycle mode power of 25 kWe even with changes in materials outside the core.

We find that fuel temperatures must be very high to drive megawatt levels of power into the tie-tube circuit. Figures 8 through 10 show calculated maximum fuel temperatures for several values of power per tie tube with different center element designs and different coolants. By increasing the number of support elements to one for every two fuel elements (a near-maximum ratio), we would have more than 600 support elements in a 75,000-lb-thrust (1500-MWt) engine. For 600 support elements, 50 kW per tie tube yields 30 MWt, or perhaps 5 or 6 MWe. Figures 11 through 16 show the corresponding tie-tube conditions for the cases of Figs. 8, 9, and 10. The design difficulty can be stated fairly simply. The tie tubes are thermally insulated to limit tie-tube temperature during the open-cycle mode. The insulator, together with the gaps between the support element and insulator and between the insulator and outer tie tube are also effective in limiting heat flow during closed-cycle operation; therefore, a large ΔT between fuel and tie-tube results at power levels of interest. Furthermore, our model is extremely optimistic because it does not include the possible gap between fuel and support element. The thermal resistance of the support element insulation must be large enough to protect the tie tubes during open-cycle operations. The limiting design point is generally not at the full-power, steady-state level, but is either during engine throttling (partial power, but full temperature) or during the shutdown transient. Employing a higher-temperature material, a carbon-carbon composite, for example, for the support structure would allow less insulation; however, a significant fraction of the fuel tie-tube ΔT during closed-cycle operation is in the gaps. It is worth pointing out that the gap thermal

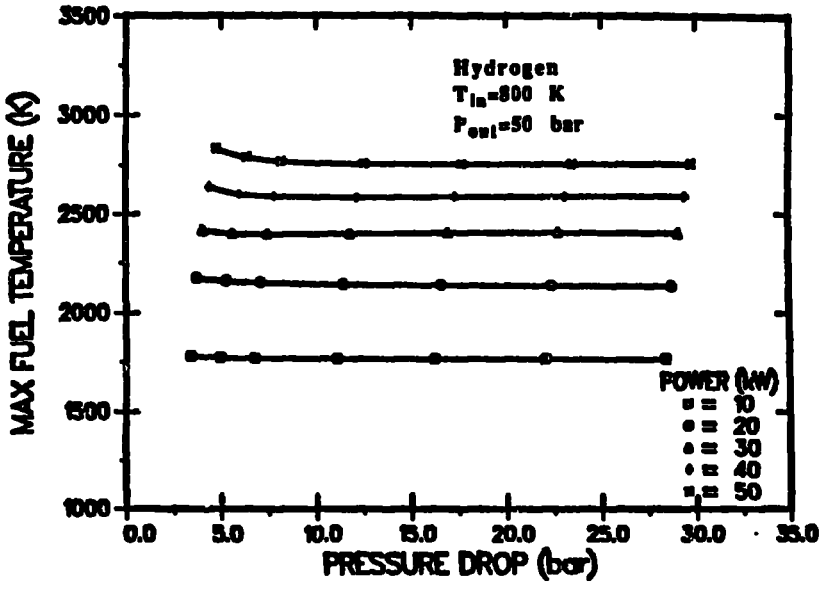

Fig. 8.
Calculated maximum fuel temperatures for several values of power per tie tube with moderator in the support element, hydrogen coolant.

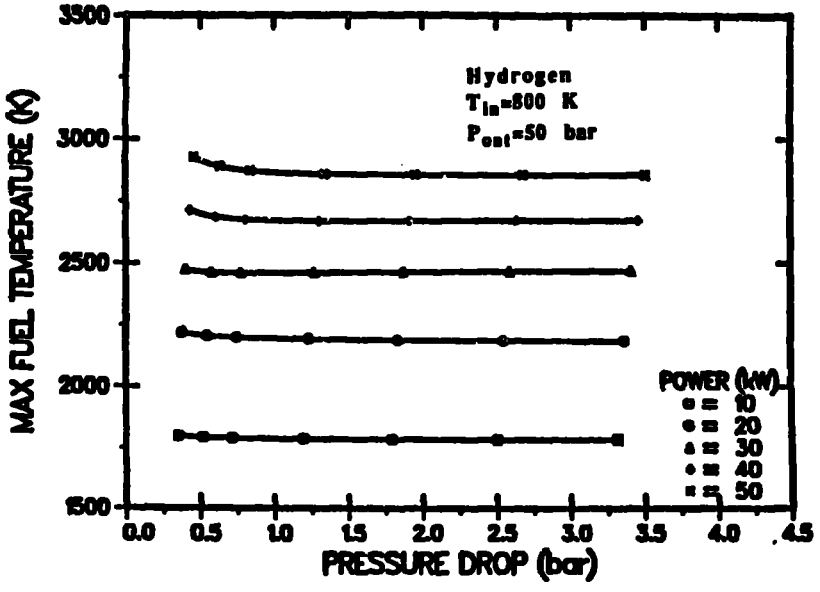

Fig. 9.
Calculated maximum fuel temperatures for several values of power per tie tube with no moderator in the support element, hydrogen coolant.

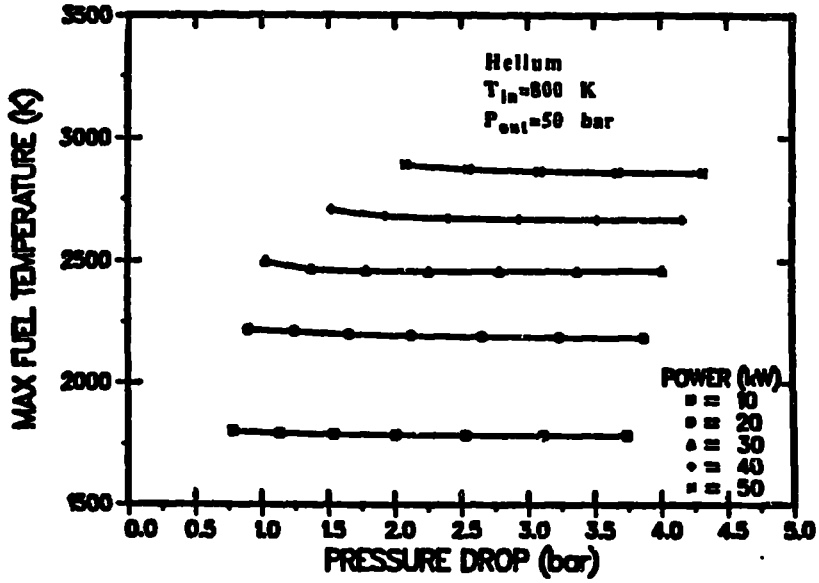

Fig. 10.
Calculated maximum fuel temperatures for several values of power per tie tube with no moderator in the support element, helium coolant.

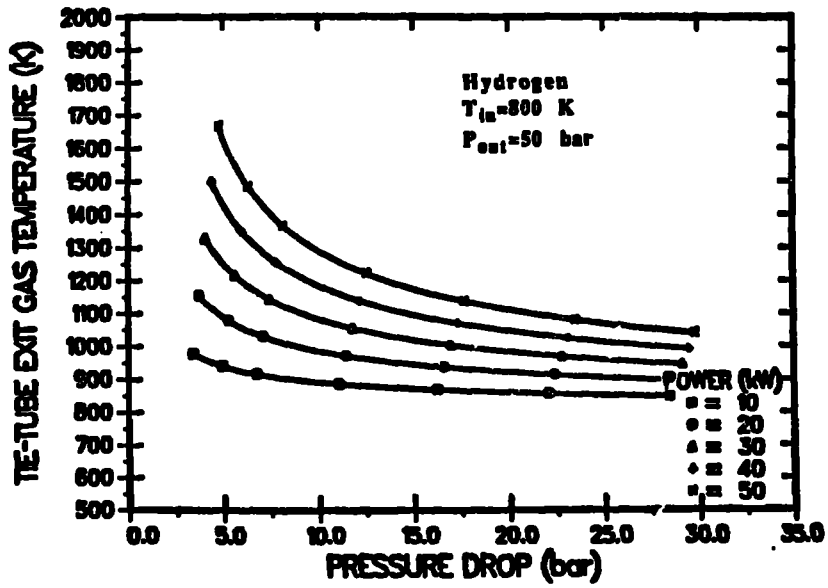

Fig. 11.
Tie-tube exit gas temperatures for case of Fig. 8.

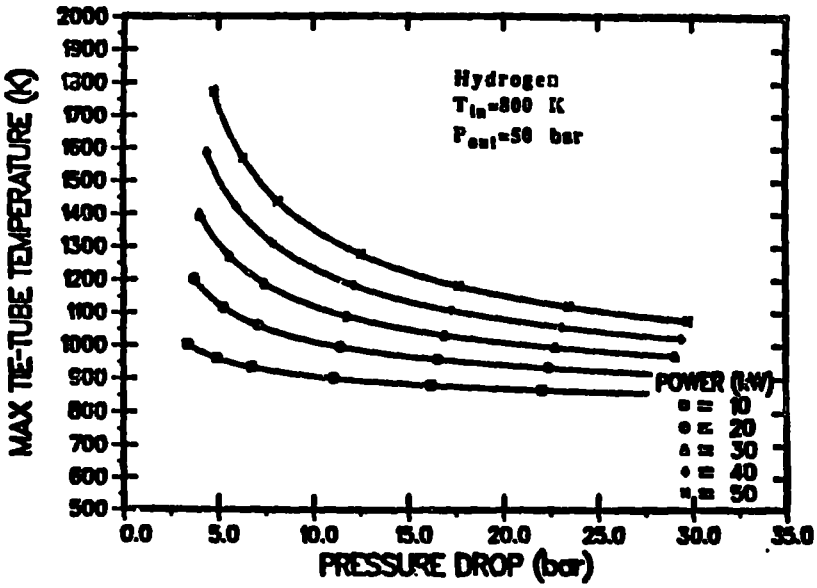

Fig. 12.

Maximum tie-tube temperatures for case of Fig. 8.

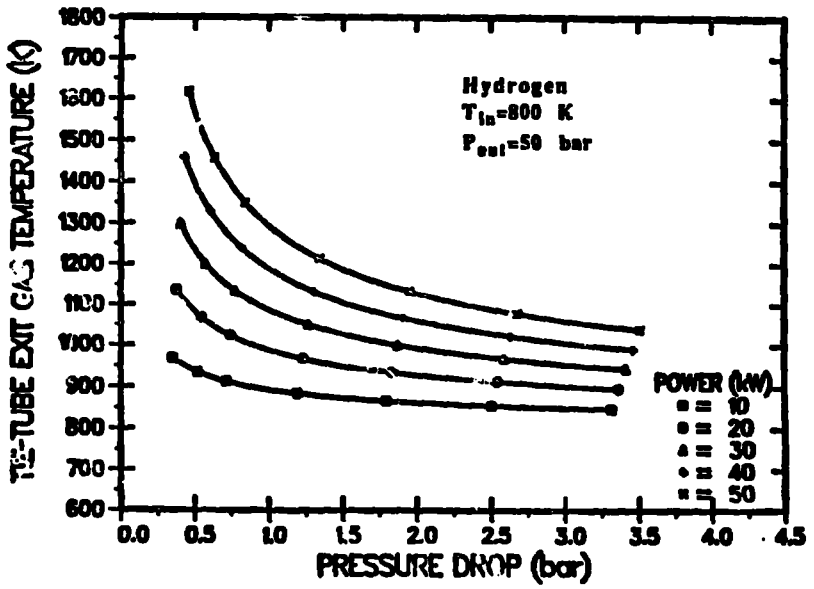

Fig. 13.

Tie-tube exit gas temperatures for case of Fig. 9.

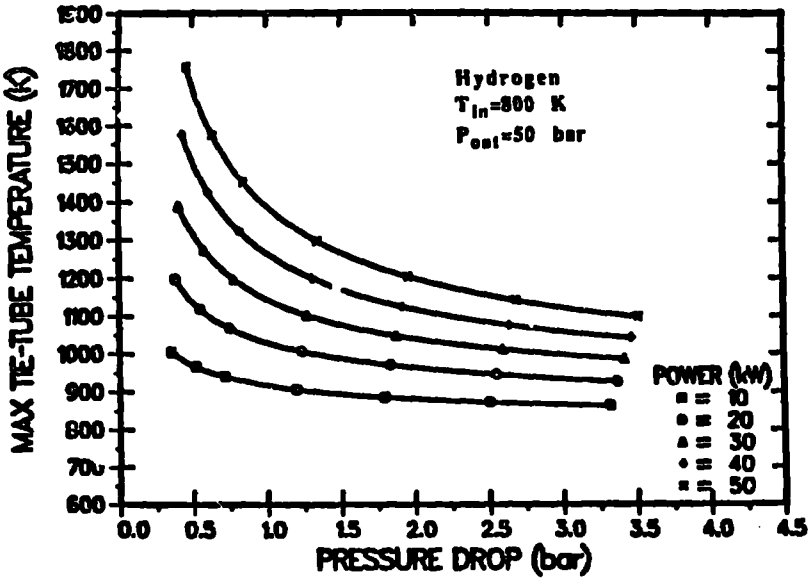

Fig. 14.

Maximum tie-tube temperatures for case of Fig. 9.

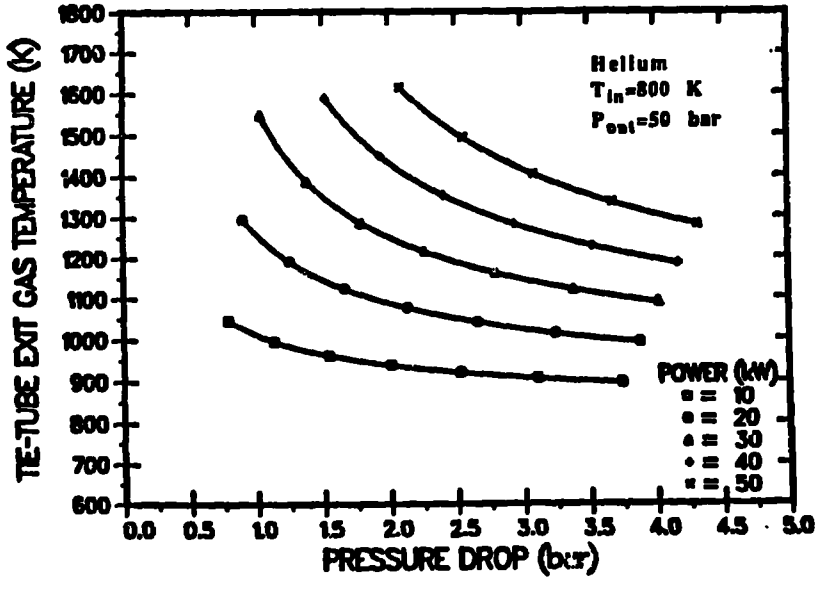

Fig. 15.

Tie-tube exit gas temperatures for case of Fig. 10.

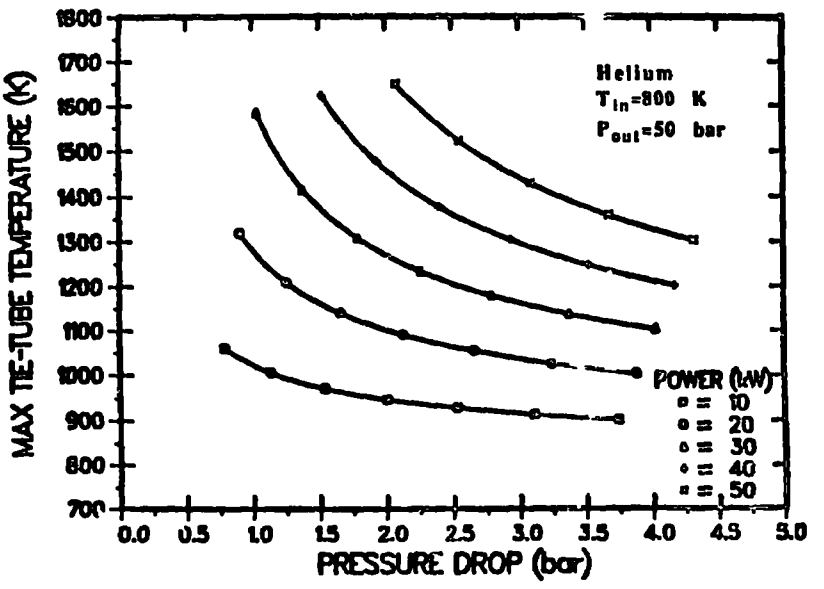

Fig. 16.
Maximum tie-tube temperatures for case of Fig. 10.

conductivity is higher when the gap contains hydrogen, as it does during open-cycle operation. Bill Pierce of Westinghouse has suggested that it might be possible to provide a low-pressure hydrogen environment in the core during closed-cycle operation by using a nozzle block. This block would be much easier to implement than the high-pressure block needed in the direct flow path scheme discussed in Sec. II.A.

The effect of low-pressure hydrogen in the gaps is quite dramatic, as shown by comparison of Fig. 10 with Fig. 17. Figure 17 shows fuel temperatures with low-pressure hydrogen in the gaps, whereas Fig. 10 represents the case of no conducting gas in the gaps. Of course there is reason for concern regarding large temperature differences across the conducting gaps that are likely to be nonuniform in practice. Therefore, there could be large uncertainties in heat flow and temperatures, which is usually an undesirable situation.

The principal concern about high fuel temperatures during the closed-cycle mode is that high fuel temperature drives large quantities of heat into other regions of the reactor and the nozzle. This heat, added to the heat generated in these components by neutrons and gamma rays, will tend to produce high material temperatures, or require direct cooling of these components, or both. Rough calculations, which yield the results shown in Fig.18, indicate that thermal radiation from the surface of a titanium pressure vessel (all Rover reactors had aluminum pressure vessels) will remove only 220 kW, but the heat generated by nuclear radiation outside the core is about 725 kW

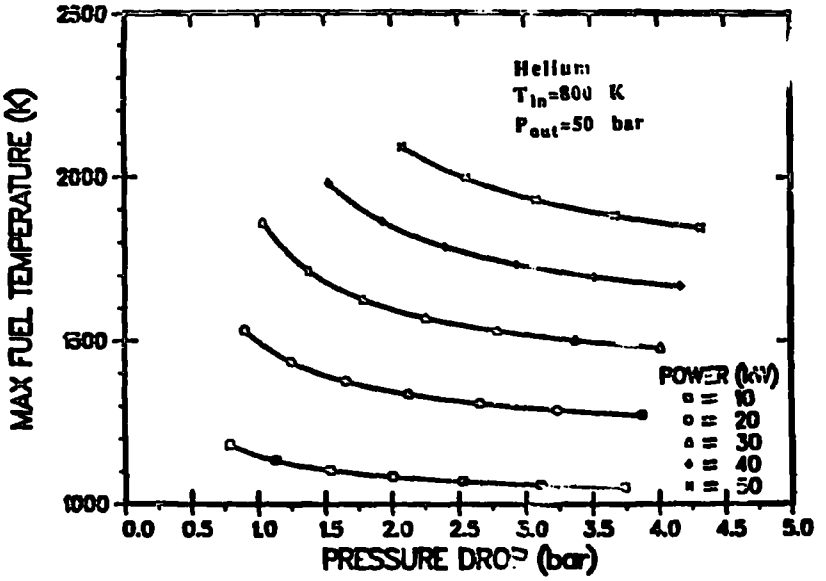

Fig. 17.

Calculated maximum fuel temperatures with hydrogen in gaps compared with Fig. 10.

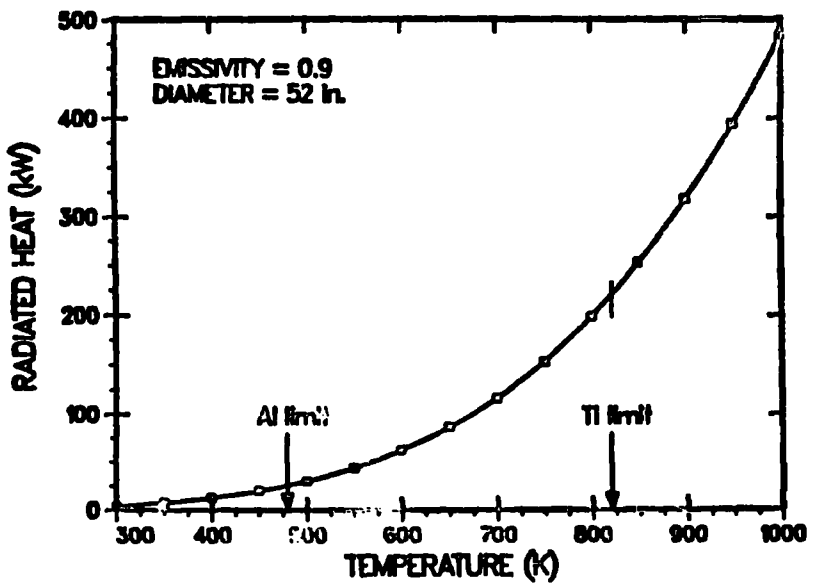

Fig. 18.

Estimate of the thermal radiation from the surface of an aluminum or a titanium pressure vessel.

at a reactor thermal power of 30 MW. Therefore, it is clear that cooling of some or all noncore components during megawatt-level closed-cycle operation will be required.

Another concern related to long-term, high-temperature operation of the fuel is possible thermally induced degeneration of the fuel. Even without hydrogen present, there will be significant interdiffusion and chemical interactions among fuel materials if the fuel is at sufficiently high temperatures. These effects may be of particular of concern if the reactor is to be used again in the open-cycle mode after operating in the closed-cycle mode.

We have considered, but not analyzed, two coolant schemes for the noncore regions of the reactor during closed-cycle operation, which are shown in Figs. 19 and 20. Figure 19 puts reflector coolant in series with the tie-tube/periphery coolant, which requires a manifold to collect the reflector effluent before it gets to the fuel flow passages. Such a manifold might be a standard feature of the open-cycle design, if full reactor flow is used to drive the H_2 turbopump. On the other hand, if the turbopump can be driven with just the energy picked up by tie-tube/periphery flow, the pressure vessel will see a much lower pressure during open-cycle operation. We do not yet know which flow scheme is better for the open-cycle design. The Fig. 19 scheme minimizes radiator and flow system mass, but requires a core inlet manifold and exposes all noncore components to relatively high coolant inlet temperatures during closed-cycle operation, based on the same arguments as those in Sec. II.A. Figure 20 shows a scheme in which separate cooling is provided for the reactor externals. The power removed in this separate circuit is rejected to space by a separate, possibly low-temperature, radiator. The coolant passages could be the same ones used during open-cycle operation (requiring a core inlet region manifold, as discussed above) or different ones that are unused during open-cycle operation. The Fig. 20 arrangement may require large auxiliary radiator and flow system masses, but has a major potential advantage in the decoupling of reflector, etc., temperatures from the main closed-cycle loop. Keeping temperatures low in these components avoids extensive changes in materials of proven reliability in the noncore reactor components.

C. Special Unfueled Elements

Because we found that high fuel-temperature levels are required to force heat through the support element insulator into the tie-tube circuit, we considered using special unloaded core elements that would have no function during open-cycle operation, but would provide a two-pass circuit for heat pickup in the closed-cycle mode. In fact, these elements would have no cooling during open-cycle operation, which means that they must be designed to include only very high-temperature materials. In simplest form, they consist of a single-hole, unloaded hexagonal element housing a high-temperature tubular flow separator. A hot-end tip that connects the inner and outer flow passages is glued/brazed to the element and separator. A major problem for this concept is coolant leakage through the element wall during closed-cycle operation. Another is the possible

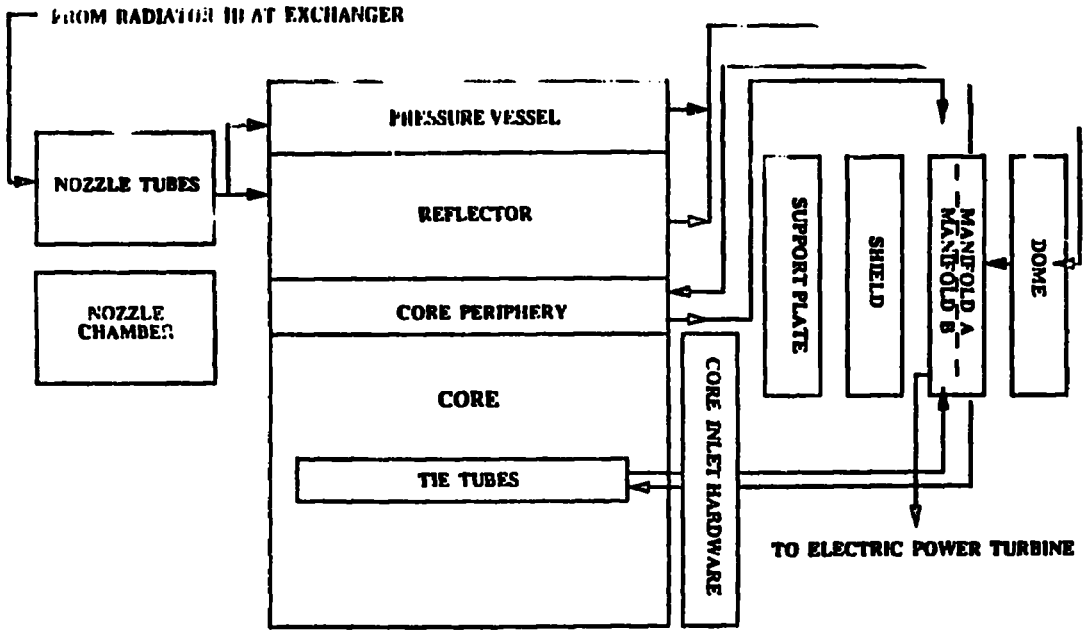

Fig. 19.

Block diagram of external region cooling in series with the tie tubes and periphery cooling.

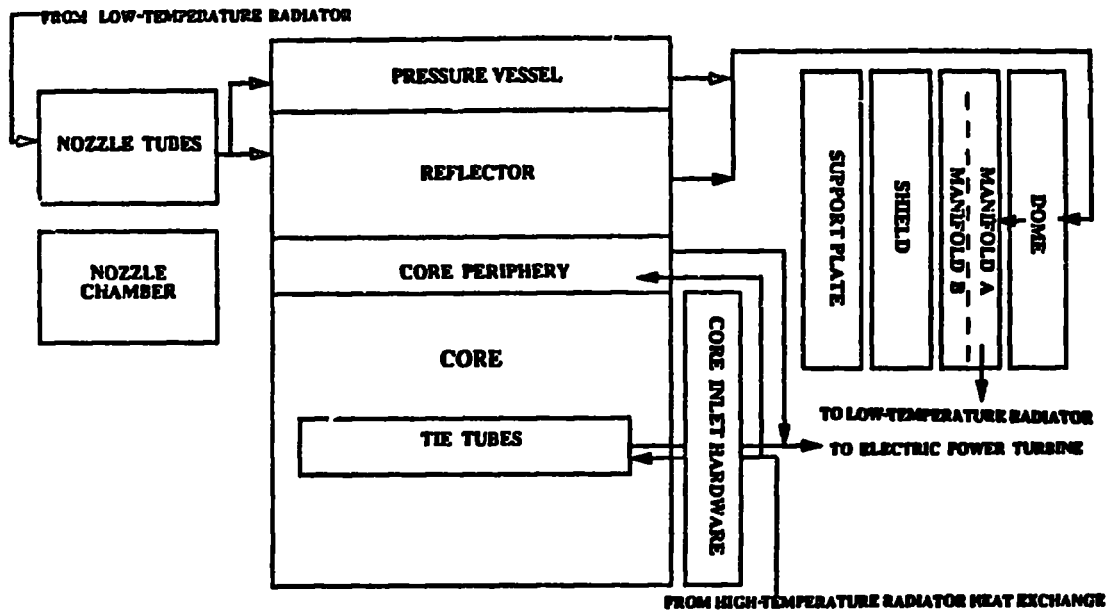

Fig. 20.

Block diagram of separate cooling circuit for external regions.

overheating (by nuclear radiation) of the flow separator during open-cycle operation. Also, the special elements increase core volume, which in turn increases engine mass because several components (for example, reflector, pressure vessel, and nozzle) would have a larger diameter. However, the concept does substantially reduce fuel temperature during closed-cycle operation. Figures 21 and 22 show some performance parameters for the individual special element when cooled by hydrogen. Figures 23 and 24 show the same parameters when the coolant is helium.

Again, there are possibilities of cooling other reactor regions either in series or in parallel with the special element circuit. Figures 25 and 26 show two possible closed-cycle flow schemes.

D. In-Core Heat Pipes

In-core heat pipes are a potential alternative approach for heat extraction from the reactor core. The principal advantage resulting from the use of heat pipes is that they are more readily and efficiently coupled to a Rankine cycle energy-conversion system. This is an important advantage, since nearly all space power system studies over the past 30 years indicate a power system mass reduction of a factor of 3 or more for a Rankine cycle as opposed to a Brayton cycle. In implementation the in-core heat pipes would be arranged much like the tie tubes, with hexagonal heat pipes replacing one of every seven fuel elements.

The in-core heat pipes must be capable of delivering thermal energy to the Rankine cycle working fluid during the closed-cycle mode while maintaining functional integrity during the open-cycle mode. That is, the heat pipes must not dry out or otherwise fail during the open-cycle mode when the reactor core is required to heat hydrogen to 2500-3100 K. Without in-core heat transfer due to the presence of the heat pipes, fuel temperatures would range from 800 K at the core inlet to 2700-3200 K near the core exit. The heat pipe is an efficient passive thermal transport device that will respond to this gradient by transferring heat in the direction of the temperature gradient within the core. Thus, there is a tendency for the heat pipes to reduce the desired high temperature at the reactor core exit. The degree to which this occurs is strongly dependent upon how the heat pipe is thermally coupled to the core. It would be desirable to decouple the heat pipes to the greatest extent possible during the open-cycle mode. However, during the closed-cycle mode of operation, it is desirable to couple the heat pipes to the fuel as well as is practical to reduce the required fuel operating hot-spot temperature. The predictability and adjustability of the thermal coupling are important in assuring heat pipe performance at the proper level during the life of the system in an operating environment that involves thermal cycling.

The closed-cycle power generation requirement has been estimated as 5-10 MWe. At an energy-conversion efficiency of 25%, the thermal power load from the reactor will be as high as 40 MWt. The heat pipe is a passive heat-transfer element that responds, within a performance envelope defined by internal heat transport limits, to the external temperature and heat flux

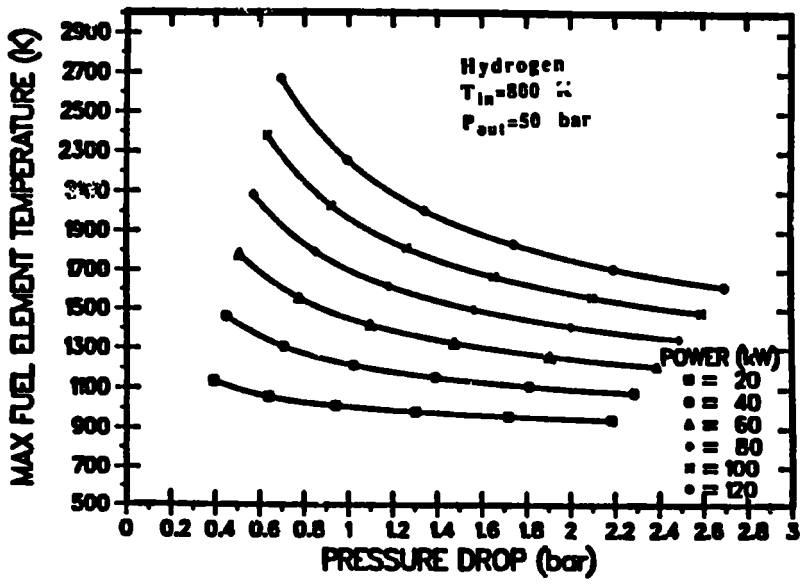

Fig. 21.
Maximum fuel temperatures using special elements at various closed-cycle power levels, hydrogen coolant.

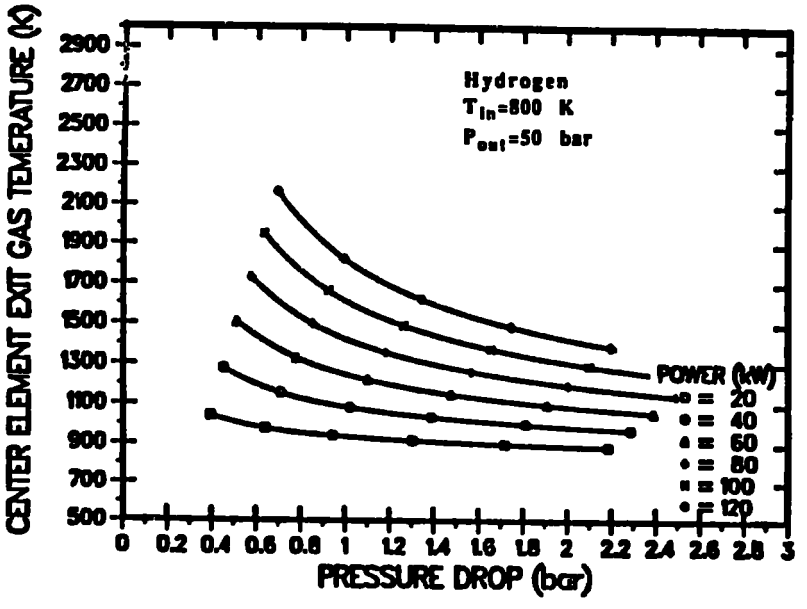

Fig. 22.
Special element exit gas temperatures for Fig. 21 cases.

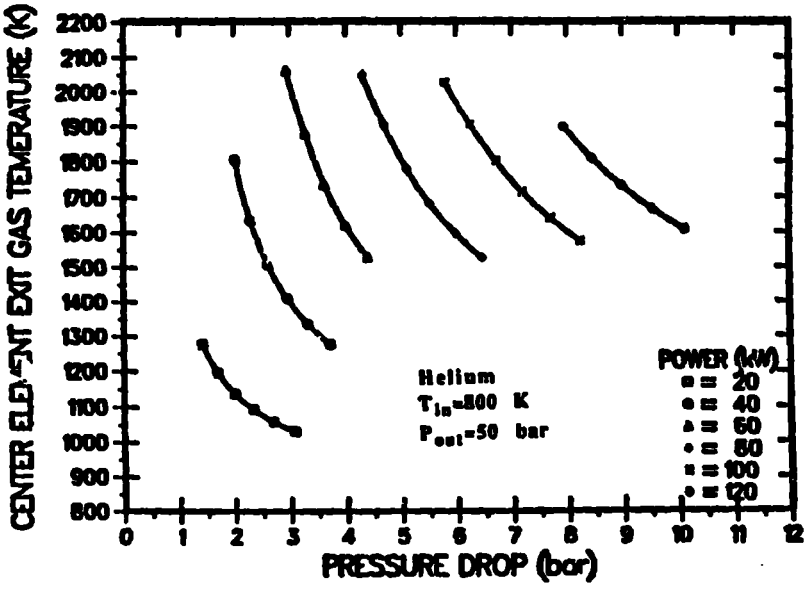

Fig. 23.
Maximum fuel temperatures using special elements at various closed-cycle power levels, helium coolant.

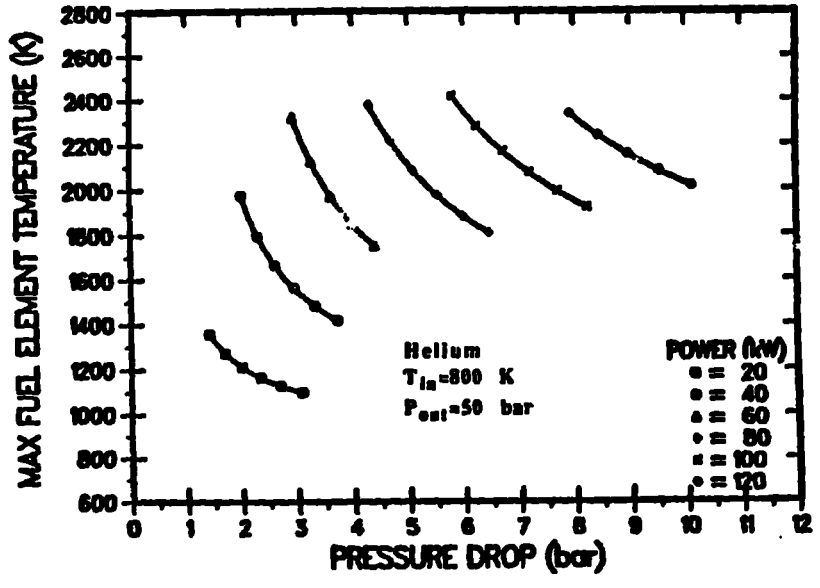

Fig. 24.
Special element exit gas temperature for Fig. 23 cases.

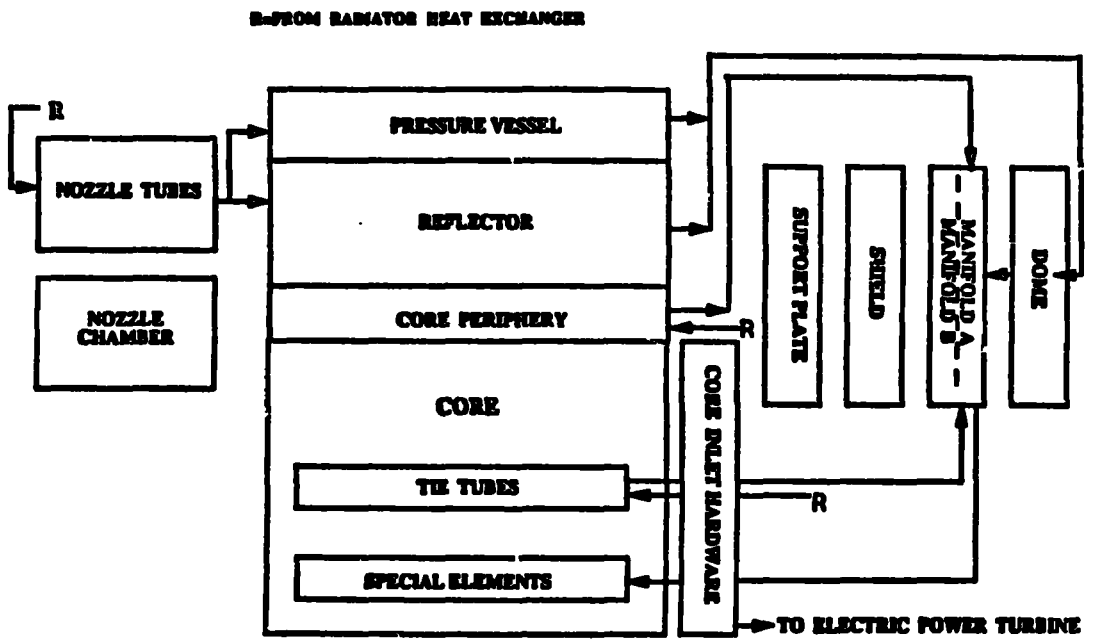

Fig. 25.
Block diagram of flow paths using special elements and parallel cooling of other reactor regions.

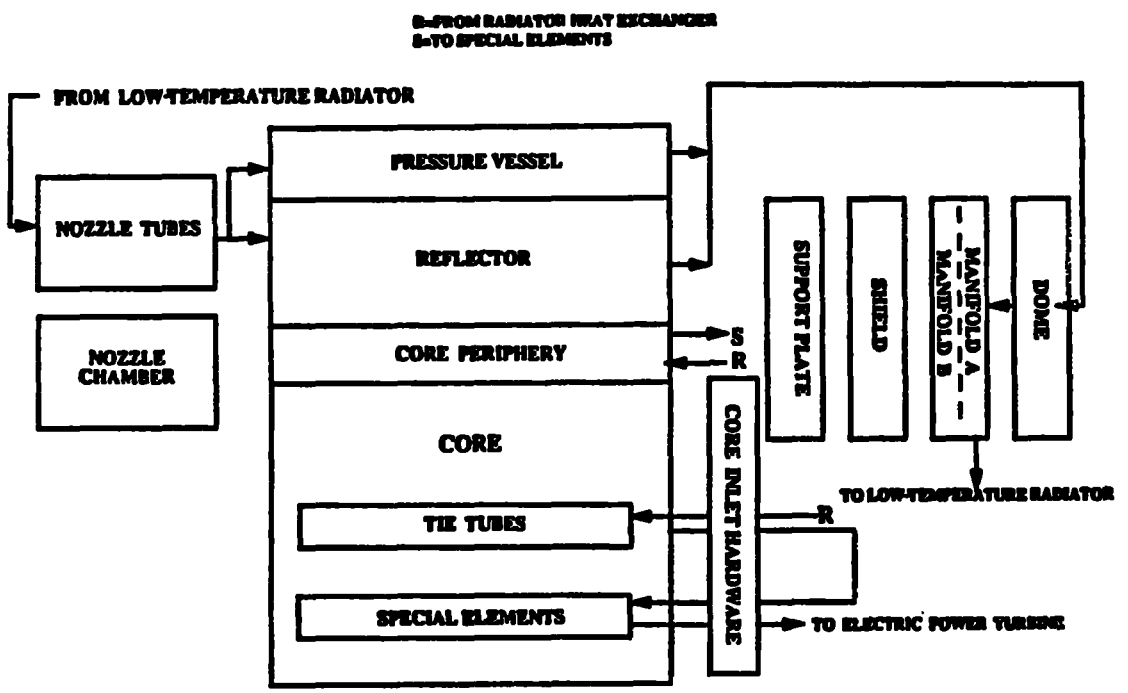

Fig. 26.
Block diagram of flow paths using special elements and series cooling of other reactor regions.

boundary conditions. For this application, there are five parameters that influence the heat transport: (1) the fuel temperature, (2) the heat pipe-to-fuel coupling, (3) the energy-conversion temperature (heat pipe sink temperature), (4) the heat pipe coupling to the energy-conversion system, and (5) the heat pipe condenser length. It is not the intent of this report to provide a parametric mapping of the possible heat pipe designs that may be suitable. Rather, a single, somewhat arbitrary example will be given to illustrate both the degree of concept feasibility and the necessary compromises.

Perhaps the most viable and practical method of decoupling the heat pipe from the core during thrust mode is to provide a physical gap between the heat pipe and the fuel elements. This gap would be evacuated during open-cycle operation so that heat transfer to the heat pipe would be by radiation alone. During closed-cycle operation, the gap would be filled with a conducting medium for improved coupling. Practical considerations dictate that the conductive medium be a gas. The gas of choice for this application is H_2 because the system will be designed for H_2 tolerance, there will be an adequate supply of H_2 available, and H_2 is the highest conductivity gas. If an inert gas was necessary, it would be the logical gas because of its high conductivity. However, the relative coupling would be reduced by 37%. We have not devised a method for providing this pattern of gap conditions. The natural behavior is the exact reverse, with H_2 in the gap during open-cycle operation.

To meet performance requirements during the closed-cycle mode, it is important to keep the gap as small as possible A practical lower limit under normal circumstances is about 10 mil (2.5×10^{-4}m). In this application, core swelling and the coefficients of expansion of the fuel and heat pipe materials would affect the gap specification. For the present calculation, a 10-mil gap is assumed.

Tables I-A and I-B present a summary of input and the resulting output generated by HTPIPE, the Los Alamos steady-state heat pipe analysis program, for a lithium heat pipe that is coupled to the fuel by a gas gap. The fuel temperature is taken as 1800 K and the heat pipe is assumed to reject heat at the condenser end to a liquid metal by forced convection. The heat pipe geometry is detailed in the table. The heat pipe is limited to 42.6 kW by the evaporator coupling. A 40-MWt system would require 940 of these heat pipes. Figure 27 shows the performance limit curves for this heat pipe.

During the open-cycle mode, the heat pipe temperature will rise to about 1750 K. With the gas removed from the gap surrounding the heat pipe, heat transfer to the heat pipe, with the core at 2700 K, would be 9.3 kW by radiation. This heat transfer would tend to lower the temperature of the fuel near the heat pipe elements. A detailed analysis would be required to predict the temperature profiles in the fuel. If this effect is significantly deleterious, one solution would be to leave some length of reactor core at the hot end with no heat pipes. Heat removal from the hot end

TABLE I-A

LIT[illegible] HEAT PIPE INPUT FOR HTPIPE

Input Parameters	
Geometry:	Circular arteries
Working fluid:	Lithium
Source coupling:	Convective
Sink coupling:	Convective
Source temperature:	1800 K
[illegible]perature:	1400 K
Evaporator length:	100 cm
Adiabatic length:	0 cm
Condenser length:	30 cm
Tilt angle:	0° (0° to 90°, positive for assist)
Pipe inside radius:	0.81 cm
Distribution screen thickness:	0.035 cm
Wick permeability:	0.18000e-06 cm^2
Half of wick diameter:	0.001 cm
Artery wick thickness:	0.01 cm
Artery inside radius:	0.1 cm
Effective pore radius, liquid/vapor interface:	0.0032 cm
Number of arteries:	4
Heat-transfer coefficient, source to pipe:	0.31 W/cm^2 K
Heat-transfer coefficient, sink to pipe:	5 W/cm^2 K
Wick surface porosity:	0.5
Thermal conductivity, pipe wick:	0.7 W/cm^2 K
Thermal conductivity, pipe wall:	0.7 W/cm^2 K
Site radius:	0.0001 cm (if 0.0, defaults to 0.00127)
Pipe outside radius:	0.96 cm
Vapor passage area:	1.73487 cm^2
Total liquid flow area:	0.12566 cm^2

TABLE I-B
SUMMARY OF OUTPUT GENERATED BY HTPIPE

Distance Along Pipe (cm)	Local Power (W)	Vapor Temp. (K)	Vapor Pressure (Pa)	Viscous Vapor Pressure Drop (Pa)	Inertial Vapor Pressure Drop (Pa)	Total Vapor Pressure Drop (Pa)	Liquid Pressure Drop (Pa)
0	0	1548	64231	0	0	0	0
20	8427	1547	64003	25	204	228	54
40	16869	1546	63314	99	818	917	129
60	25358	1543	62147	224	1860	2084	228
80	33924	1540	60469	403	3360	3763	348
100	42606	1535	58222	639	5370	6009	492
106	34263	1537	59247	790	4194	4984	664
112	25785	1539	60066	892	3273	4166	831
118	17200	1540	60664	955	2613	3568	993
124	8538	1541	61028	986	2217	3203	1149
130	-171	1541	61145	998	2088	3086	1300

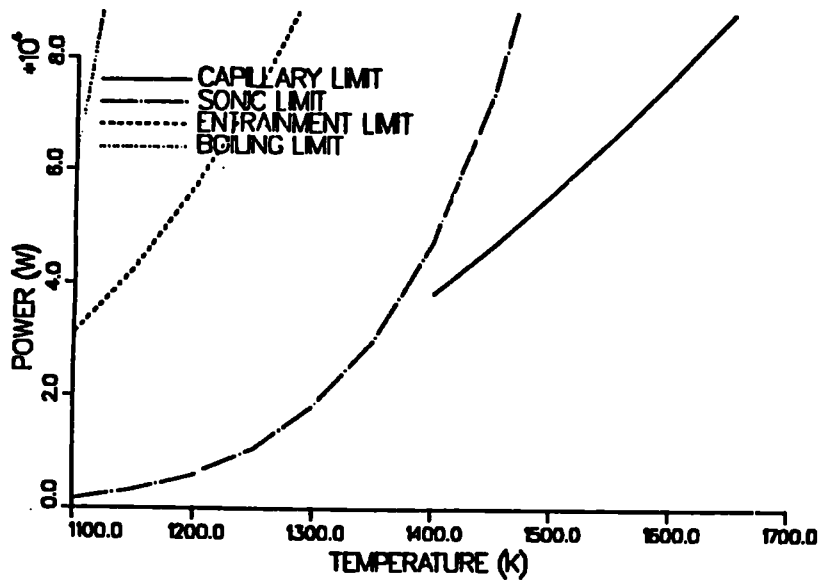

Fig. 27.
Performance limit curves for heat pipe.

of the core during closed-cycle operation would then depend on axial conduction and thermal radiation to the nozzle. No calculations have been performed for this geometry, but the heat transfer to the heat pipe from the core would be reduced in proportion to its length reduction.

In-core heat pipes can, in theory, provide a means of heat transfer to a Rankine cycle energy-conversion system. However, accommodating dual-mode operation would require significant innovations in system design in order to obtain good performance during both open- and closed-cycle modes.

III. SYSTEM ANALYSIS

It is necessary to predict the mass of the high-power dual-mode system, in addition to investigating its design in order to judge its worth in comparison with separate reactor systems. A priori, it was expected that the mass of separate propulsion and power systems would be competitive with the dual-mode system (especially at higher electric power levels). This section contains a comparison of mass estimates for several propulsion/power systems using either dual-mode (one reactor) or independent (two reactors) heat sources.

A large number of dynamic energy-conversion systems are appropriate for high power levels (in a minimum mass sense). The challenges involved in designing the power-conversion subsystem are both similar to and different than those involved in designing an independent, high-

power space nuclear power system. They are similar in that once the thermal energy is acquired from the heat-generation point (whether it be a rocket reactor or a power reactor), the thermodynamic energy-conversion cycle requires the same components in the balance of plant for both systems. The design of the dual-mode subsystem, however, must take into account the requirements for both modes of operation, which may impose restrictions on the choice of reactor coolant and reactor coolant inlet and outlet state points for the closed-cycle mode. These differences translate into additional mass over the mass of an independent space nuclear power system of the same power level. Although there are in theory many possible energy-conversion schemes, the major possibilities are as follows:

(1) dual-mode direct Brayton or potassium Rankine cycles
(2) dual-mode indirect potassium Rankine cycle
(3) independent direct Brayton
(4) independent direct or heat pipe coupled potassium Rankine cycle
(5) independent thermionic system

Of the dual-mode concepts, we have excluded all but the direct Brayton cycle from consideration. We have not yet found any plausible method of directly heating potassium in a dual-mode reactor that must also heat hydrogen to 3000 K in its open-cycle mode nor have we been able to devise a believable way to use heat pipes to transport heat from the reactor to the potassium working fluid. A gas-potassium heat exchanger seems technically possible (but likely very massive) and may deserve further consideration in later studies. Because of these doubts about the feasibility of dual-mode potassium Rankine systems, we chose to focus only on the direct Brayton dual-mode system. Of the separate reactor systems considered for producing electrical power, we have focused on the direct Brayton cycle because of its similarity to the dual-mode direct Brayton cycle. We also considered the direct potassium Rankine cycle because of its potential low mass but reserved the thermionic system for later studies.

To simplify the discussion, the following terms are defined:

- M_1 is the mass of an unmodified (baseline) nuclear-thermal rocket without shielding.
- ΔM_1 is the mass increment required to use the baseline nuclear-thermal rocket in a closed mode as a heat source for electrical power generation (for propulsion).
- S_1 is the mass of the shielding (both internal and external) of the baseline nuclear-thermal rocket .
- ΔS_1 is the mass increment in shielding required to operate the baseline nuclear-thermal rocket also in the closed-cycle mode.

- M_2 is the mass of an independent nuclear reactor serving only as a heat source for electrical power generation (for propulsion).
- S_2 is the mass of shielding required for an independent reactor heat source
- C is the mass of a power-conversion subsystem of an independent nuclear power system.
- ΔC is the mass increment of the power-conversion subsystem required because of operation limits imposed by the dual-mode reactor.

It is assumed that the power control, conditioning and distribution subsystem, and electrical thruster masses are not affected by the heat source configuration and that optimum nuclear thermal rocket power (and therefore M1) is the same for either independent or dual-mode configurations. From the definitions above, the mass of a dual-mode system = $M_1 + \Delta M_1 + S_1 + \Delta S_1 + C + \Delta C$ and the mass of an independent reactor system = $M_1 + S_1 + M_2 + S_2 + C$.

In order to facilitate the analysis of the Brayton dual-mode system, values of independent nuclear-electric power system component masses from the literature were used as a basis and were further supplemented with simple modeling and scaling calculations. There is, understandably but unfortunately, a large variation in performance predictions for nuclear-electric power systems in the literature, with an increasing dispersion at higher electrical power levels. Sandia National Laboratories (SNL) and NASA's Lewis Research Center (Lewis) have completed a comprehensive study[4-6] of various multimegawatt nuclear-electric systems and the Mission Analysis Panel at the 1990 NTP/NEP Workshops[7] chose some representative specific mass values for nuclear power system components. Mass information from these sources is shown in Table II and Fig. 28. To supplement this information, radiator mass as a function of electrical power, turbine inlet temperature, and radiator mass per unit area was calculated using a lumped-parameter model that was benchmarked against the SNL-Lewis values at 10 MWe. Figure 29 was then constructed by assuming that the total mass of all non-radiator power-conversion subsystem components varied linearly with power (based on Fig. 28). This figure provides a value for C, as defined above, for any particular set of power-conversion system parameters and can also be used to estimate ΔC if, for instance, the dual-mode reactor gas exit temperature is less than that of an independent reactor. A similar analysis could be but has not been done to estimate a ΔC effect for limitations on the dual-mode reactor inlet temperature (subsequently, $\Delta C = 0$ is assumed).

Estimating shielding mass is extremely difficult. The first intuitive thought is that reduced total shielding mass is a major advantage of a dual-mode system. However, more consideration of the matter leads to a realization that there are many factors that affect shield mass. Both the dual-mode and the independent reactor shields may have multiple purposes. For example, the NERVA nuclear rocket engine internal shield was sited primarily to protect engine components and to

TABLE II
COMPONENT SPECIFIC MASSES FOR A 10-MWE MAN-RATED POWER SYSTEM (FROM REF. 7)

Subsystem	Specific Mass (kg/kWe)
Reactor	1.2
Shield	1.8
Power Conversion	2.4
Main Radiators	1.0
Power Conditioning and Distribution	2.5

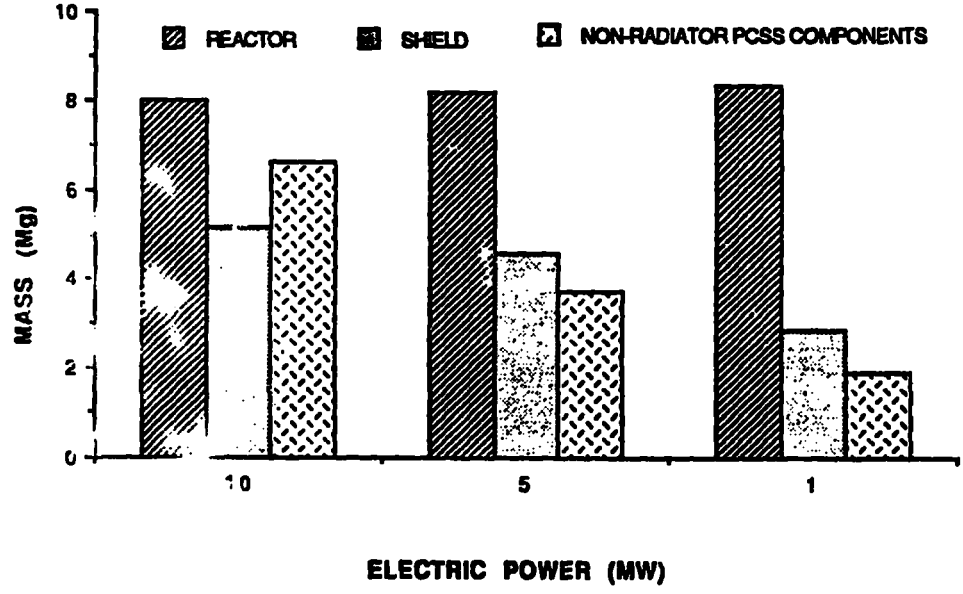

Fig. 28.
Brayton component mass as a function of electric power level (from Ref. 6).

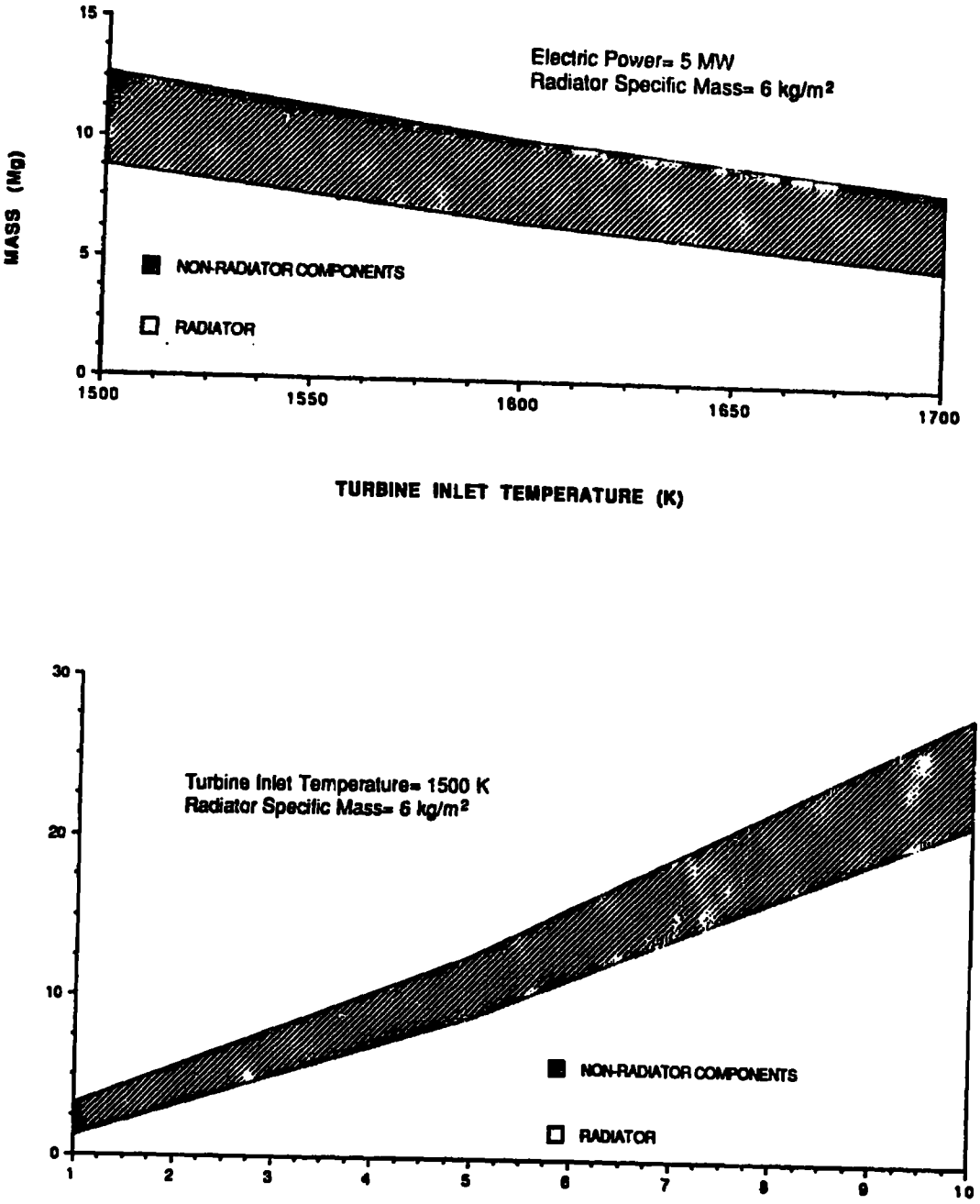

Fig. 29.
Brayton cycle power-conversion subsystem mass as a function of electric power level and turbine inlet temperature.

reduce propellant heating. A second external shield was to be incorporated to protect the payload for a specific mission. Current thoughts, however, suggest that shielding to protect the engine and propellent may not be necessary because of advances in materials technology since 1972. Furthermore, if thick payload shielding against space radiation is needed, then perhaps no additional payload protection in the form of reactor shielding is necessary. These same arguments, perhaps less persuasively, can be extended to a nuclear-electric system. In the context of our mass nomenclature mentioned above, S1 is assumed to be about 6000-7000 kg for a typical nuclear rocket engine with about one-third of the mass in an internal shield.[8] To be conservative, we assumed a specific mass of 1.8 kg/kWe in estimating S_2. Unfortunately, it is not as easy to estimate ΔS_1 for all cases, particularly if the cross-sectional area of the dual-mode reactor is large compared with that of the independent reactor. In calculating a range of ΔS_1, it is assumed that $(\Delta S_1 + S_1)$ is at least the larger of S_1 or S_2 and at most is this same minimum plus some fraction of S_1 (which again, is a linear function of the electric power level). These assumptions and the final shield mass estimates are summarized in Tables III and IV, respectively.

Mass estimates for the dual-mode and independent reactors were obtained in a similar manner. M_1 has been estimated (Ref. 8) to be 8200 kg for the reference rocket engine. Approximate values of M_2 are indicated in Fig. 28. Note that the mass of gas-cooled reactors varies little over the 1- to 10-MWe range because gas-cooled reactors are criticality and not heat transfer limited. Our engineering judgment anticipates ΔM_1 to increase as the required electrical power level increases, but the exact shape of this dependence is unknown. However, as an example, a linear variation of ΔM_1 vs electrical power level was assumed in order to complete the mass comparison of the dual-mode and independent reactor systems. Table III contains the assumptions and ranges used to arrive at the values in Table IV, which summarizes the mass estimates for both a dual-mode Brayton system (both high and low estimates) and an independent Brayton system. To complete the preliminary assessment, values for M_2 and C for an independent direct potassium Rankine system were obtained (Ref. 9) and combined with values for M_1, S_1, and S_2 to yield Fig. 30, which summarizes the mass competitiveness of the dual-mode direct Brayton system with independent Brayton and potassium Rankine systems. From this figure it can be seen that the Brayton dual-mode system may be mass competitive with an independent Brayton or Rankine system, but the degree to which it is depends on the mass impact of design changes to the reactor (ΔM_1) and shield (ΔS_1).

IV. SUMMARY AND CONCLUSIONS

Starting with an assumption that dual-mode propulsion will be advantageous for a high ΔV mission such as a manned mission to Mars, we have studied several concepts for using the same

TABLE III
ASSUMPTIONS USED TO CALCULATE COMPONENT MASSES FOR DUAL-MODE AND INDEPENDENT NUCLEAR PROPULSION/POWER SYSTEMS

Component or Subsystem		Assumptions		
		Power = 1 MWe	Power = 5 MWe	Power = 10 MWe
Dual-Mode:	M_1	8.2 Mg (from Ref. 8)		
	ΔM_1	10% of M_1 ⇔ 100% of M_1	50% of M_1 ⇔ 150% of M_1	100% of M_1 ⇔ 200% of M_1
	S_1	6.5 Mg (from Ref. 8)		
	ΔS_1	greater of S_1 and S_2 less S_1 ⇔ same plus 10% of S_1	greater of S_1 and S_2 less S_1 ⇔ same plus 50% of S_1	greater of S_1 and S_2 less S_1 ⇔ same plus 100% of S_1
	C	from Fig. 29		
	ΔC	assumed to be negligible		
Independent:	M_2	from Fig. 28		
	S_2	1.8 kg/kWe (from Ref. 7)		
	C	from Fig. 29		
	M_1	same as dual-mode system		
	S_1	same as dual-mode system		

reactor as the heat source for both nuclear-thermal and nuclear-electric propulsion. Our goal was to provide some basis for judging the merits of using one reactor vs using two, one for each mode. Our s. "es to date have been quite limited in detail, but do show some significant problems in adapting a nuclear-thermal engine reactor to closed-cycle operation, particularly at higher electrical power levels. The simplest and most generally attractive closed-cycle concept has a closed-cycle coolant flow path through the reactor identical to the open-cycle flow path. The nozzle is blocked and the coolant is diverted through the nozzle wall. All reactor regions are cooled, but the reactor inlet coolant temperature is much higher than during open-cycle operation, which probably requires compromises in materials for the reflector, pressure vessel, and core inlet regions.

TABLE IV
COMPONENT COMPARISON OF DUAL-MODE AND INDEPENDENT PROPULSION/POWER SYSTEMS

Component or Subsystem		Component Mass (Mg) Power = 1 MWe	Power = 5 MWe	Power = 10 MWe
Dual-Mode:	M_1	8.2	8.2	8.2
	ΔM_1	0.82 ⇔ 8.2	4.1 ⇔ 12.3	8.2 ⇔ 16.4
	S_1	6.5	6.5	6.5
	ΔS_1	0.0 ⇔ 0.65	2.5 ⇔ 5.75	11.5 ⇔ 18.0
	C	3.16	12.6	27.8
	ΔC	0.0	0.0	0.0
Total		18.68 ⇔ 26.71	33.9 ⇔ 45.75	62.2 ⇔ 76.9
Independent:	M_2	8.0	8.0	8.0
	S_2	1.8	9.0	18.0
	C	3.16	12.6	27.8
	M_1	8.2	8.2	8.2
	S_1	6.5	6.5	6.5
Total		27.66	44.3	68.5

Using the tie tube or similar secondary core coolant circuits to collect energy originating in the fuel will work well at lower powers, but becomes much less attractive at higher power because the heat flow is limited and controlled by imprecise gaps between the core components. Active cooling of noncore regions will be necessary at higher powers.

Introducing heat pipes into the core to extract heat for electrical power production leads to so-far unresolved problems with heat pipe survival at open-cycle core conditions.

Energy conversion and heat rejection analyses provide estimates of the potential mass saving by using one reactor instead of two. Two reactors allow more flexibility in the choice of reactor coolant and conversion cycle; however, dual-mode operation may reduce reactor and shielding mass. The mass comparisons of this study are inconclusive.

We tentatively conclude that separate reactors are a better choice if tens of thermal megawatts are required during closed-cycle operation. Dual-mode operation for either power or propulsion will be more feasible and more advantageous at lower power levels.

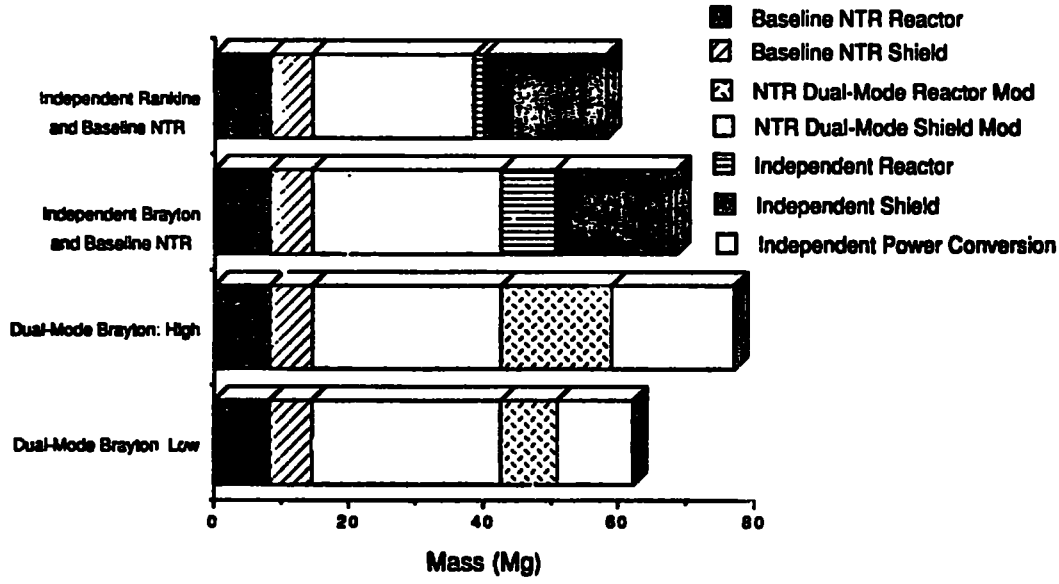

Fig. 30.

Mass comparison of 10-MWe dual-mode and independent nuclear propulsion/power systems. NTR = nuclear-thermal rocket.

REFERENCES

1. J. H. Beveridge, "Feasibility of Using the NERVA Rocket Engine for Electrical Power Generation," AIAA/SAE Paper No. 712-639, 7th Propulsion Joint Specialist Conference, Salt Lake City, Utah, June 14-18, 1971.
2. L. A. Booth and J. H. Altsheimer, "LA-DC-1111 Summary of Nuclear Engine Dual-Mode Electrical Power System Preliminary Study," Los Alamos Scientific Laboratory document (October 1972).
3. J. P. Layton, J. Grey, and W. Smith, "Preliminary Analysis of a Dual-Mode Nuclear Space Power and Propulsion System," AIAA Paper No. 77-512, Conference on the Future of Aerospace Power Systems, St. Louis, Missouri, March 1-3, 1977.
4. A. C. Marshall, "A Review of Gas-Cooled Reactor Concepts for SDI Applications," Sandia National Laboratories report SAND87-0558 (August 1989).
5. A. J. Juhasz and B. I. Jones, "Analysis of Closed Cycle Megawatt Class Space Power Systems with Nuclear Reactor Heat Sources," in *Trans. 4th Symposium on Space Nuclear Power Systems*, CONF-870102, Albuquerque, New Mexico, January 12-16, 1987.

6. "Space Power Technology—Short Course Series Notes," Institute for Space Nuclear Power Studies, University of New Mexico, January 5-8, 1989.
7. National Aeronautics and Space Administration, "NEP/NTP Workshop Steering Committee Report—Mission Analysis Panel Report," Lewis Research Center, Cleveland, Ohio. September 18, 1990.
8. Los Alamos National Laboratory, Westinghouse Advanced Energy Systems, and Rockwell Rocketdyne, presentation to NASA Marshall Flight Center, March 21-22, 1990.
9. Rockwell International, Rocketdyne Division, "Ultra-High-Power Space Nuclear Power System Design and Development," NASA Contract NAS325808 final report (November 1989).